Nuclear-Structure Studies in Mo and Nb Isotopes via Stripping Reactions at 12 MeV*

J. B. MOORHEAD† AND R. A. MOYER
Department of Physics, University of Pittsburgh, Pittsburgh, Pennsylvania 15213
(Received 14 October 1968; revised manuscript received 20 February 1969)

Proton energy spectra from (d, p) reactions induced by 12-MeV deuterons on targets of Mo^{92}, Mo^{94}, Mo^{98}, and Nb^{93} were measured with 7–9-keV resolution. Angular distributions of proton groups in the spectra were used to determine the l values of the transitions yielding the respective proton groups. In reactions on the Mo isotopes, all of the expected strength is found for transitions leading to $s_{1/2}$, $d_{3/2}$, and $d_{5/2}$ states. In contrast with the situation in the isotonic Zr isotopes, where no $h_{11/2}$ states are known, one $h_{11/2}$ state is found in each odd-A Mo isotope; however, in each case the excitation strength is only a small fraction of the expected total for that level. The total excitation strength for the $g_{7/2}$ level is also far below the expected total, and there is no evidence that this level is filling in the Mo isotopes as neutrons are added. In Nb^{94}, values of I for several members of the $(\pi g_{9/2})(\nu d_{5/2})$ and $(\pi g_{9/2})(\nu g_{7/2})$ configurations are estimated from sum rules and the presence of mixing.

INTRODUCTION

THIS is the third paper in a series of high-resolution studies of nuclear structure in nonclosed-shell nuclei in the $N=50$–82 shell via the (d, p) reaction. In the first paper of this series,[1] studies of two odd-A palladium isotopes were reported. In the second paper,[2] the odd-A nucleus Cd^{115} and the odd-odd nucleus In^{116} were investigated. In this paper, we report on three more odd-A nuclei, Mo^{93}, Mo^{95}, and Mo^{99}, and the odd-odd nucleus Nb^{94}. Comparisons of these isotopes with their respective isotones of Zr, which are well understood,[3] and comparisons between Nb^{94} and Mo^{95}, which are also isotones, are made here.

Experimental studies of (d, p) reactions on the Mo isotopes have been reported by Hjorth and Cohen,[4] but due to their resolution, only the strongly excited peaks were identified. The resolution in the present experiment, 7–9 keV, is nearly an order of magnitude better than that of Hjorth and Cohen. Experimental studies of (d, p) reactions on Nb^{93} have been performed by Sheline *et al.*,[5] but only the energies of the levels in Nb^{94} were reported.

EXPERIMENTAL

In the experiments reported here, deuterons at a bombarding energy of 12.0 MeV were prepared using techniques which are essentially the same as those discussed in Ref. 1. Energy spectra of scattered protons were analyzed using an Enge split-pole spectrograph. Target material was only deposited over a rectangle of width 0.4 mm and of height 3.0 mm in the center of the carbon backing. With targets of this type, the spot of target material provided the object for the spectrograph, thus eliminating the necessity for small slits near the target. Without these slits, background due to slit scattering was reduced in the proton spectra, and the contribution to resolution due to the divergence of the beam between the slit and target was eliminated.

The spot targets of thicknesses between 50 and 100 $\mu g/cm^2$ were prepared by using a slit to mask off all of the carbon backing except that onto which target material was to be deposited. During the experiment, initial tuning was achieved by maximizing the beam through the same slit placed in the target position. Final tuning was obtained by placing the target in position and maximizing the counting rate of the elastic peak in the monitors.

Surface-barrier detectors placed at scattering angles of $\pm 38°$ were used to monitor the incident beam by counting elastically scattered deuterons. A multichannel analyzer was used to separate the elastic peaks due to scattering from the target material and from the carbon backing. The monitoring system was used to estimate the product of (average target thickness) $\times$ (integrated beam current through the target), which is described in detail in Ref. 2. This product is proportional to the ratio of the number of counts in the deuteron elastic peak to the deuteron elastic cross section, which was obtained from tabular data.[6]

Typical beam currents measured by a Faraday cup were 1 μA. Because of the spot nature of the target, it is estimated that half of the current passed through the target material; hence, the integrated current measured by the Faraday cup was not used to calculate cross sections.

Figures 1 and 2 are typical proton spectra for the $Mo^{94}(d, p)Mo^{95}$ and $Nb^{93}(d, p)Nb^{94}$ reactions at labo-

* Work supported by National Science Foundation.
† Presently at the Nuclear Defense Laboratory, Edgewood Arsenal, Md.
[1] B. L. Cohen, J. B. Moorhead, and R. A. Moyer, Phys. Rev. **161**, 1257 (1967).
[2] J. B. Moorhead, B. L. Cohen, and R. A. Moyer, Phys. Rev. **165**, 1287 (1968).
[3] B. L. Cohen and O. V. Chubinsky, Phys. Rev. **131**, 2184 (1963).
[4] S. A. Hjorth and B. L. Cohen, Phys. Rev. **135**, 920 (1964).
[5] R. K. Sheline, R. T. Jernigan, J. B. Ball, K. H. Bhatt, Y. E. Kim, and J. Vervier, Nucl. Phys. **61**, 342 (1965).
[6] G. Mairle and U. Schmidt-Rohr, Max Planck Institut für Kernphysik (Heidelberg) Report No. 19651 V 113 (unpublished).

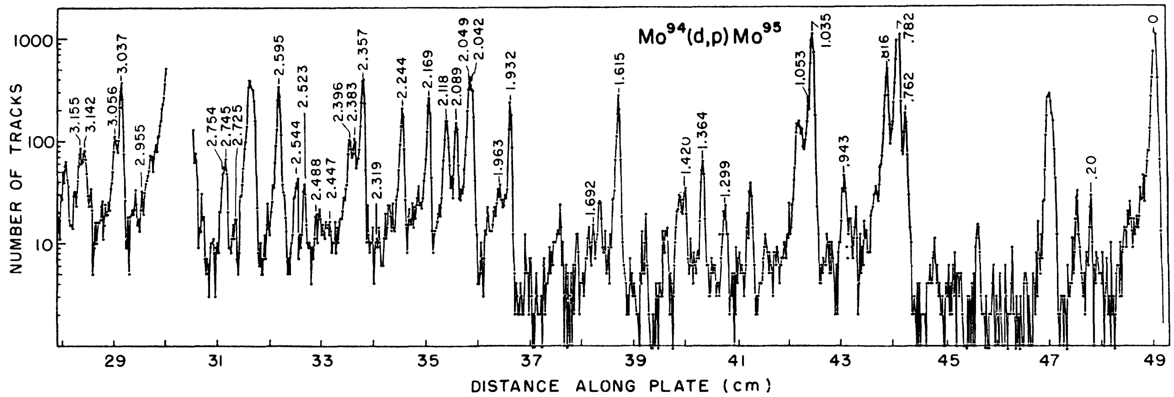

FIG. 1. Mo^{94}(d, p)Mo^{95} spectrum. Proton spectrum at 33° is representative of that for all Mo(d, p). Numbers above peaks are excitation energies of levels in Mo^{95}.

ratory scattering angles of 33° and 45°, respectively. Figure 1 is representative of all of the Mo(d, p) data. Several wide, unlabeled proton groups in each spectrum are caused by the presence of light impurities in the target. Low A impurities have a broad peak shape because they are kinematically defocused by the spectrograph. The position of these peaks changes drastically and monotonically with scattering angle when compared to the remainder of the spectrum. This shift results from differences in the (d, p) kinematics for target particles of different masses. Thus, peaks of this nature were not confused with those of the isotope being studied, but they obscured useful data at some angles. Data were taken at 12 angles from 8° to 55°. In almost all cases, enough data points were available so that the proton angular distribution could be used to identify the l value of the transition leading to the proton group.

The only peaks which were not kinematically separable from the isotope being studied were those due to different isotopes of the same element that were included in the original sample used for making targets. This problem did not arise with Nb^{93}, which is monoisotopic in its natural state. The Mo^{92}, Mo^{94}, and Mo^{98} isotopes had enrichments of 97.5, 93.9, and 98.3%, respectively. Although isotopic impurities were small, the transitions from an impurity with large cross sections showed more strength than weak transitions from the isotope being studied. The proton energies of the weakly excited states were compared to known strongly excited states in the other isotopes; those peaks due to impurities were disregarded.

RESULTS AND ANALYSIS

Figure 3 shows proton angular distributions predicted by distorted-wave Born-approximation[7] (DWBA) calculations with appropriate optical-model parameters[8] (given in Table I) for (d, p) reactions on Mo^{98}

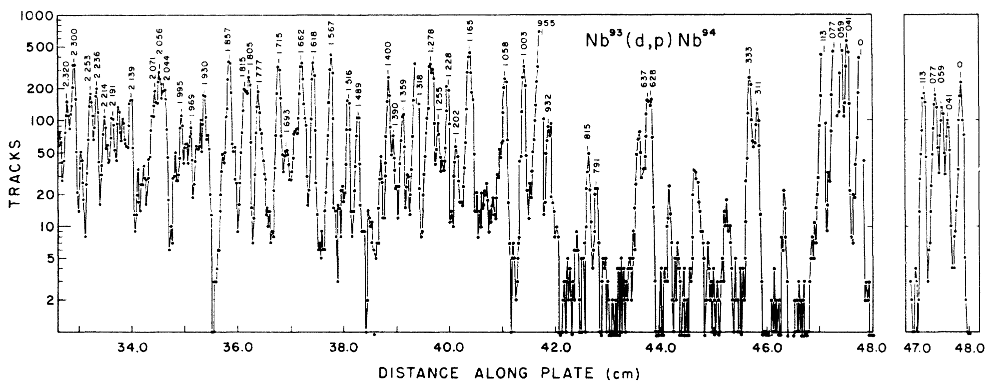

FIG. 2. Nb^{93}(d, p)Nb^{94} spectrum. Numbers above peaks are excitation energies of levels in Nb^{94}. Detached portion of spectrum is an exposure of the ground-state quintuplet, which is included because those peaks are over exposed in the full spectrum at left. Angle of detection is 45°.

[7] R. H. Bassel, R. M. Drisko, and G. R. Satchler, Oak Ridge National Laboratory, memorandum on JULIE code (unpublished).

[8] For the Mo calculations no deuteron optical-model parameters were available at 12 MeV and no proton parameters were available at any energy. Mo elastic scattering data resemble Pd and Rh data more closely than they resemble Zr and Nb data. In the Mo calculation, Pd deuteron optical-model parameters are used, since a complete set for Rh is not available at 12 MeV. However, Rh proton parameters are used in the Mo calculation. Table I lists the parameters used.

TABLE I. Optical-model parameters used in the DWBA calculations.

	V (MeV)	r_0 (fm)	r_c (fm)	a (fm)	W (MeV)	r_0' (fm)	a' (fm)	V_{so} (MeV)
				Deuteron				
Mo (Pd)	77.7	1.322	1.322	0.654	37.2	1.213	0.617	···
Nb	95.5	1.201	1.201	0.687	18.2	1.24	0.661	···
				Proton				
Mo (Rh)	57.66	1.15	1.25	0.687	8.206	1.263	0.738	8.16
Nb	50.6	1.25	1.25	0.678	14.1	1.25	0.47	8.0

and Nb^{93}. All of those shown are for a Q value of 4.0 MeV except Nb^{93} with $l=5$, which is for $Q=3.0$ MeV. The angular distributions corresponding to an l-value transfer of 0 are forward peaked with a secondary maximum between 30° and 33°. Those for $l=2$ are peaked from 20° to 25°. The $l=4$ transitions have angular distributions peaked between 39° and 43°. Those angular distributions corresponding to $l=5$ transitions are peaked from 50° to 55°. Although they are not shown, angular distributions for $l=1$ and 3 were calculated and have primary peaks at about 15° and 30°, respectively. The l value of each transition was determined by comparing experimental angular distributions with those predicted by DWBA.

For (d,p) reactions, the spectroscopic factor S_{jk} for a transition with a transfer of total angular momentum j is given by

$$\frac{d\sigma}{d\Omega_{jk}}=\frac{2I_B+1}{2I_A+1}S_{jk}\sigma_j(\text{DWBA}), \tag{1}$$

where $d\sigma/d\Omega_{jk}$ is the cross section to the state with a total angular momentum transfer of j; the index j also includes the quantum numbers n and l, and the index k labels the particular transition among those with the same quantum number j. The spins of the initial and final nuclei are given by I_A and I_B respectively. For a target with an even number of neutrons, the probability that the single-particle level characterized by j is empty is given by

$$U_j^2=\sum_k S_{jk}=S_j. \tag{2}$$

For targets with an even number of protons as well as neutrons, I_A and I_B reduce to 0 and j, respectively. Thus, S_{jk} is given by

$$d\sigma/d\Omega_{jk}=(2j+1)S_{jk}\sigma_j(\text{DWBA}). \tag{3}$$

For a target with an odd number of protons, I_B is not well defined so that a new factor for each transition should be defined as

$$S_{jk}'=\frac{2I_B+1}{(2I_A+1)(2j+1)}S_{jk}. \tag{4}$$

In this case, S_{jk}' is independent of I_B and Eq. (1) reduces to

$$d\sigma/d\Omega_{jk}=(2j+1)S_{jk}'\sigma(\text{DWBA}). \tag{5}$$

Using the above equations, the following relationship is obtained

$$S_j'(I_B)=\sum_k S_{jk}'(I_B)=\frac{2I_B+1}{(2I_A+1)(2j+1)}U_j^2, \tag{6}$$

for given final spin I_B. Finally, this yields

$$S_j'=\sum_{I_B}S_j'(I_B)=\frac{U_j^2}{(2I_A+1)(2j+1)}\sum_{I_B}(2I_B+1)=U_j^2. \tag{7}$$

Hence for odd-proton even-neutron targets, S_j' has the same significance as S_j does for even-even targets.

Transitions of $d_{3/2}$ and $d_{5/2}$ can be distinguished by the following considerations: For (d,t) reactions on targets with an even number of neutrons, S_j can be related to the single-particle state's degree of fullness by

$$S_j(d,t)\sim(2j+1)V_j^2, \tag{8}$$

where

$$V_j^2=1-U_j^2.$$

Shell-model theory predicts that the $d_{5/2}$ level lies lower and is hence fuller than the $d_{3/2}$ level. Thus,

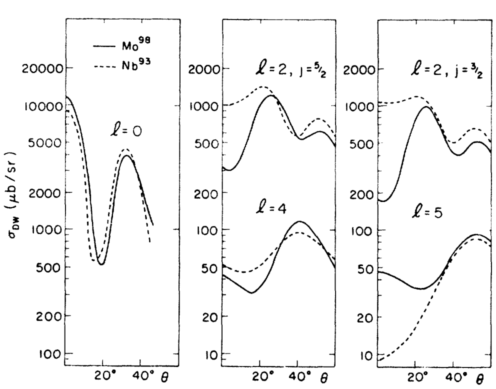

FIG. 3. Absolute DWBA calculated angular distributions of (d,p) cross sections for targets of Nb^{93} and Mo^{98}.

TABLE II. Levels in Mo^{93} from (d, p) reactions. Included are the energies, angular momenta, and parities of the neutron levels, along with (d, p) cross sections and spectroscopic factors of the transitions leading to them.

Present work							Previous work[a]			
E (MeV)	l	j^{π}	$(d\sigma/d\Omega)$ (d, p)[b] (mb/sr)	$S(d, p)$	$S(d, t)$[c]	$S(d, t)/S(d, p)$[d]	E (MeV)	l	j^{π}	$S(d, p)$
0.0	2	5/2+	5.90	0.84	1.0	1.2	0.0	2	5/2+	0.87
0.940	0	1/2+	4.65	0.64			0.944	0	1/2+	0.70
1.359	4	7/2+	0.314	0.26						
1.489	2	3/2+	2.62	0.50	0.05	0.10	1.486	2	3/2+	0.43
	2	(5/2+)	0.409	(0.051)						
1.516					0.37					
	4	7/2+	0.178	0.14						
1.691	2	3/2+	0.970	0.18	0.020	0.11	1.695	2	5/2+	0.074
2.175	2	3/2+	0.323	0.053			2.186	(2)	3/2+	0.083
2.301	(5)	11/2−	0.565	0.33			2.300	4	7/2+	0.37
2.394	2	3/2+	0.278	0.043						
2.434	0	1/2+	0.765	0.071			2.445	0	1/2+	0.15
2.534										
2.664	0	1/2+	0.100	0.009						
2.699	0	1/2+	3.64	0.32			2.700	0	1/2+	0.030
2.833	0	1/2+	0.305	0.026						
							2.850	2	3/2+	0.087
2.874	3	(7/2−)	0.416	0.047						
2.966										
3.019	4	7/2+	0.072	0.047						
3.059										
3.151	2	3/2+	1.09	0.20			3.155	2	3/2+	0.15
3.201										
							3.426	2	3/2+	0.13
							3.586	2	3/2+	0.10
							3.693	2	3/2+	0.083

[a] See Ref. 4.
[b] Cross section measured at first peak beyond 10°.
[c] Relative spectroscopic factor.
[d] Relative ratio.

the ratio

$$\frac{S_j(d,t)}{S_j(d,p)} \sim \frac{(2j+1)V_j^2}{U_j^2}, \tag{9}$$

should be much larger for $d_{5/2}$ transitions than for $d_{3/2}$ transitions. To distinguish the $d_{3/2}$ and $d_{5/2}$ transitions, which have similar angular distributions, (d, t) reactions were performed on the Mo isotopes yielding the same final nuclei as those being studied by (d, p) reactions. The relative ratio of $S_{jk}(d,t)/S_{jk}(d,p)$ was used to assign the values of j to $l=2$ transitions. Although Eq. (9) cannot be extended to justify the use of relative spectroscopic factor ratios for individual peaks, the technique is borne out empirically.

Results for $Mo^{92}(d, p)Mo^{93}$ Reaction

Figure 4 shows the proton angular distributions for the $Mo^{92}(d,p)Mo^{93}$ reaction grouped according to l, and Table II summarizes the results. On the basis of $Mo^{94}(d,t)$ reactions exciting the same states in Mo^{93} as does $Mo^{92}(d,p)$, the ground state of Mo^{93}, which corresponds to an $l=2$ transition, is assigned $j=\frac{5}{2}$ in agreement with previous[4] and unrelated[9] work. The 1.516-MeV level in Mo^{93} is tentatively assigned $j=\frac{5}{2}$ on this basis. The assignment is uncertain because this level is part of a closely spaced doublet

[9] *Nuclear Data Sheets*, compiled by K. Way *et al.* (Academic Press Inc., New York, 1965).

with an $l=4$ component. The 1.516-MeV level is weakly excited. (This level was not seen in Ref. 4, which was done with an energy resolution of 50 keV.) The main differences between this work and Ref. 4 are (1) there are more states seen here, (2) the 1.691-MeV level is here assigned $j=\frac{3}{2}$, whereas it was there assigned $j=\frac{5}{2}$, without (d,t) corroboration, and (3)

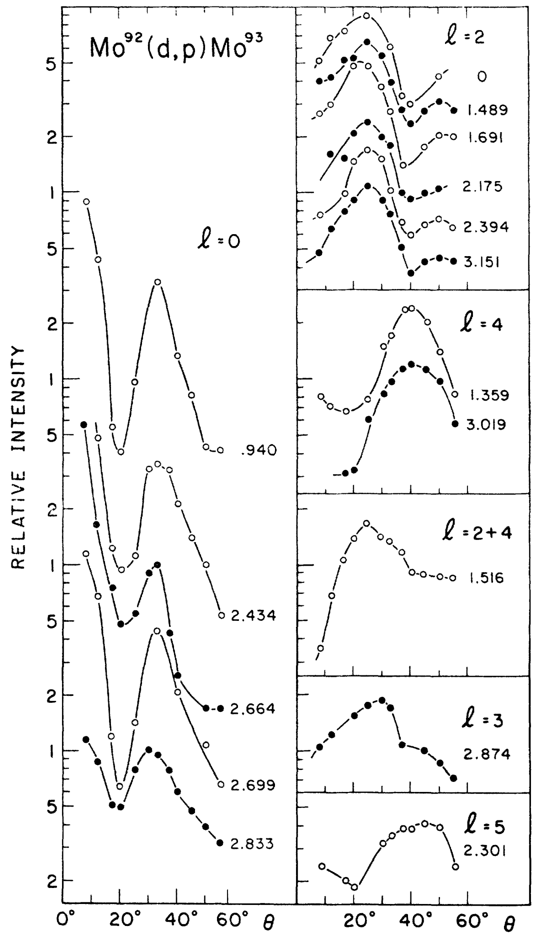

FIG. 4. $Mo^{92}(d,p)Mo^{93}$ angular distributions. Data taken at laboratory scattering angles of 8°, 12°, 17°, 20°, 25°, 30°, 33°, 37°, 45°, 50°, and 55°. Pictured are smooth curves drawn through the data points. Numbers at right are excitation energies in MeV of corresponding levels in the final nucleus.

here the 2.301-MeV level is assigned to be $\frac{11}{2}^-$ instead of $\frac{7}{2}^+$. This last level has an angular distribution which is still strong at 50° and only starts to decrease at 55°, whereas typical experimental $l=4$ angular distributions in this region have substantially decreased by 45°. Thus, the 2.301-MeV level is assigned $l=5$ and $j=\frac{11}{2}$. Figure 5 shows a plot of the spectroscopic factors for each of the levels versus excitation energy. The center of gravity and sum of spectroscopic factors are included for each single-quasiparticle level.

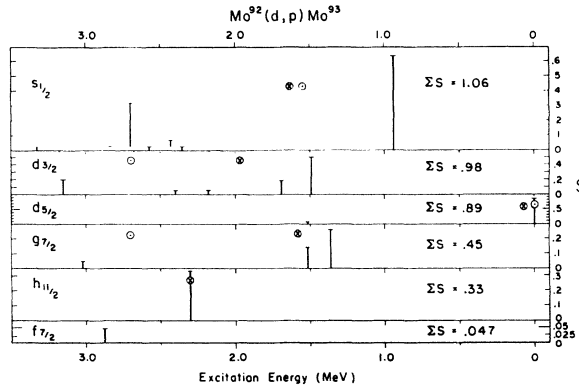

FIG. 5. Spectroscopic factors for $Mo^{92}(d,p)Mo^{93}$ reaction. The height of each vertical line is proportional to the spectroscopic factor of the transition. The distance from the right is proportional to the excitation energy in the final nucleus. Circled x's are centers of gravity of the single-quasiparticle levels. Circled dots are centers of gravity in corresponding isotone in Zr.

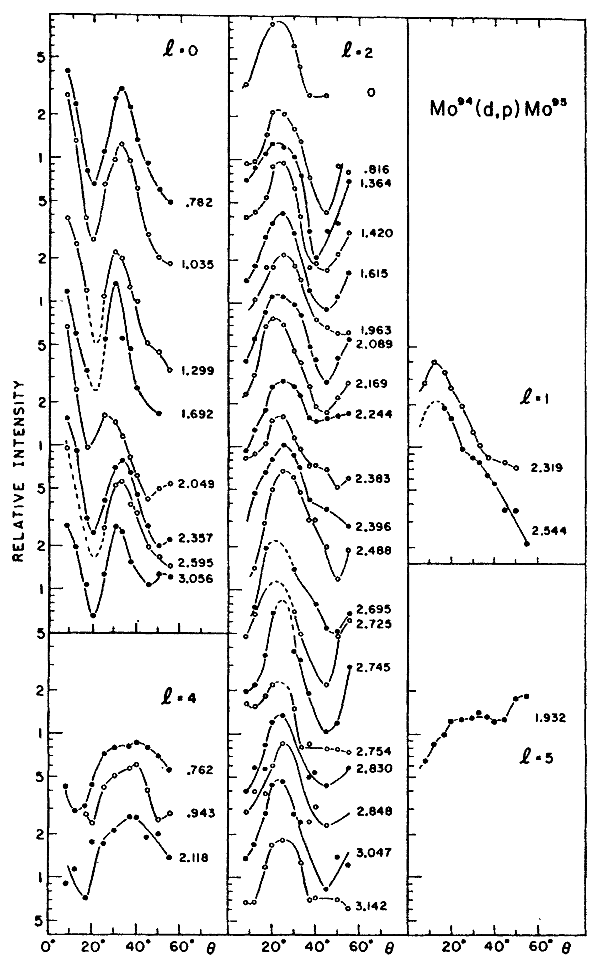

FIG. 6. $Mo^{94}(d,p)Mo^{95}$ angular distributions. See caption to Fig. 4.

TABLE III. Levels in Mo^{95} from (d, p) reactions. See caption to Table II.

Present work							Previous work[a]			
E (MeV)	l	j^π	$(d\sigma/d\Omega)$ (d, p) [b] (mb/sr)	$S(d, p)$	$S(d, t)$ [c]	$S(d, t)/S(d, p)$ [d]	E (MeV)	l	j^π	$S(d, p)$
0.0	2	$5/2^+$	4.78	0.59	1.0	1.7	0.0	2	$5/2^+$	0.74
0.202	(2)	$(3/2^+)$	0.090	0.019	0.003	0.16				
0.762	4	$7/2^+$	0.234	0.18						
0.782	0	$1/2^+$	3.28	0.37			0.806	0	$1/2^+$	0.53
0.816	2	$(5/2^+)$	1.62	0.17	0.076	0.45	0.806	2	$3/2^+$	0.32
0.943	4	$7/2^+$	0.076	0.060						
							0.970	2	$5/2^+$	0.029
1.035	0	$1/2^+$	1.190	0.19			1.055	0	$1/2^+$	0.17
1.053										
							1.277	(0)	$1/2^+$	0.03
1.299	0	$1/2^+$	0.052	0.004						
1.364	2	$3/2^+$	0.206	0.030	0.003	0.10				
							1.390	2	$5/2^+$	0.049
1.420	2	$3/2^+$	0.162	0.026	0.005	0.19				
1.615	2	$3/2^+$	0.938	0.15	0.020	0.13	1.630	2	$5/2^+$	0.11
1.692	(0)	$(1/2^+)$	0.061	0.006						
							1.80	(2)	$3/2^+$	0.042
							1.80	(0)	$1/2^+$	0.025
1.932	5	$11/2^-$	0.472	0.26			1.95	(4)	$7/2^+$	0.44
1.963	2	$5/2^+$	0.103	0.008	0.014	1.8	1.95	(2)	$3/2^+$	0.046
2.042	2	$(3/2^+)$	(0.689)	(0.10)						
2.049	0	$1/2^+$	1.12	0.097			2.08	(0)	$1/2^+$	0.045
2.089	2	$3/2^+$	0.386	0.055	0.006	0.11	2.08	(2)	$3/2^+$	0.25
2.118	4	$7/2^+$	0.166	0.11						
2.169	2	$3/2^+$	0.891	0.12	0.010	0.08	2.172	2	$3/2^+$	0.14
2.244	2	$3/2^+$	0.362	0.050	0.008	0.16	2.275	(2)	$3/2^+$	0.094
2.319	1	$(3/2^-)$	0.045	0.006						
2.357	0	$1/2^+$	0.735	0.058						
2.383	2	$3/2^+$	0.273	0.036	0.003	0.08				
2.396	2	$3/2^+$	0.309	0.040	0.004	0.10	2.39	(1)	$3/2^-$	0.098
2.447										
2.488	2	$(3/2^+)$	0.048	0.006						
2										
2.544	(1)	$(3/2^-)$	0.173	0.023			2.52	(0) (1)	$1/2^+$	0.38
2.595	0	$1/2^+$	0.730	0.055						
							2.62	(2) (1)	$3/2^-$	0.12
2.671										
2.695	(2)	$(3/2^+)$	(0.148)	0.018						
2.725	(2)	$(3/2^+)$	0.053	0.006						
							2.706	(2)	$(3/2^+)$	0.082
2.745	(2)	$(3/2^+)$	0.212	0.025						
2.754	(2)	$(3/2^+)$	0.148	0.017						
2.830	2	$3/2^+$	0.262	0.036						
							2.846	2	$3/2^+$	0.058
2.843	2	$3/2^+$	0.212	0.024						
2.919										
2.955							2.954	0	$1/2^+$	0.17
3.037	2	$3/2^+$	1.37	0.15			3.065	2	$3/2^+$	0.11
3.056	0	$1/2^+$	0.277	0.019			3.150	(1) (2)	$3/2^-$	0.027
3.142	2	$(3/2^+)$	0.276	0.031			3.150	(4)	$7/2^+$	0.045
3.155										

[a] See Ref. 4.
[b] Measured at first peak above 10°.
[c] Relative spectroscopic factor.
[d] Relative ratio.

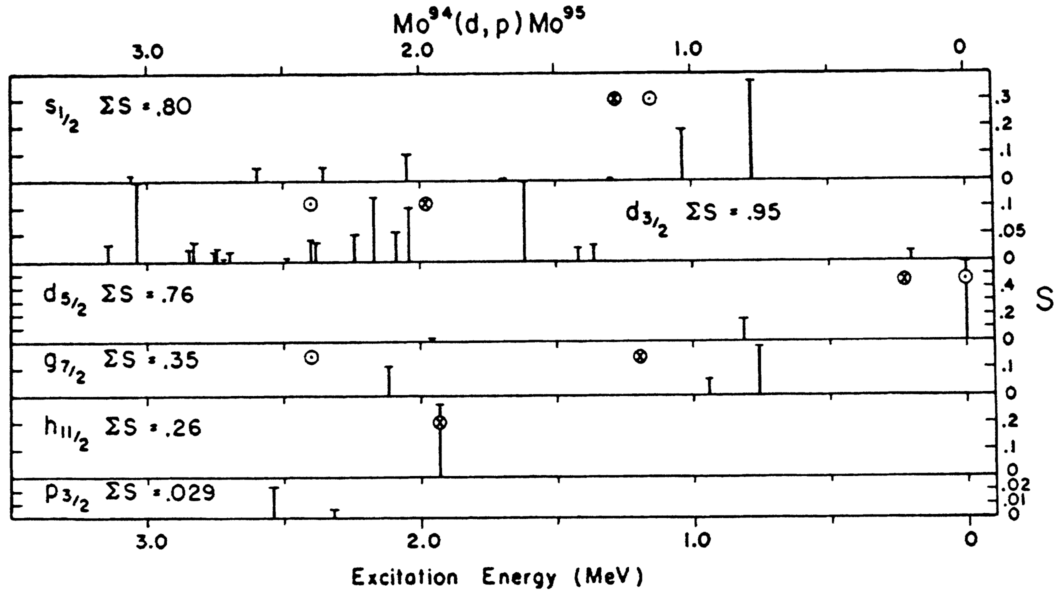

FIG. 7. Spectroscopic factors for $Mo^{94}(d, p)Mo^{95}$ reaction. See caption to Fig. 5.

The sum for the $s_{1/2}$ single-quasiparticle level is greater than unity, being 1.07. This is not surprising, since the total error in calculating S could be as large as 25% from errors in determining $d\sigma/d\Omega$ and in the DWBA approximation.

Results for $Mo^{94}(d, p)Mo^{95}$ Reaction

The angular distributions for the $Mo^{94}(d, p)Mo^{95}$ reaction are shown in Fig. 6, and the results are summarized in Table III. The results of (d, t) reactions on Mo^{96} were used to distinguish $d_{3/2}$ from $d_{5/2}$ levels. Using this technique, the ground state, the 0.816-, and the 1.963-MeV levels are assigned $j=\frac{5}{2}$. The remainder of the states resulting from $l=2$ transitions are assigned $j=\frac{3}{2}$. The ground state is in agreement with Ref. 4, but the 1.963-MeV level was assigned there $d_{3/2}$, without (d, t) corroboration. There is disagreement for the 0.816-MeV level also; from these data the most probable spin for that level is $\frac{5}{2}$. The 1.932-MeV level is here assigned $l=5$ and hence $j=\frac{11}{2}$ from the high points at 50° and 55°. The (d, p) spectroscopic factors versus energy of the levels in Mo^{95} are plotted on Fig. 7.

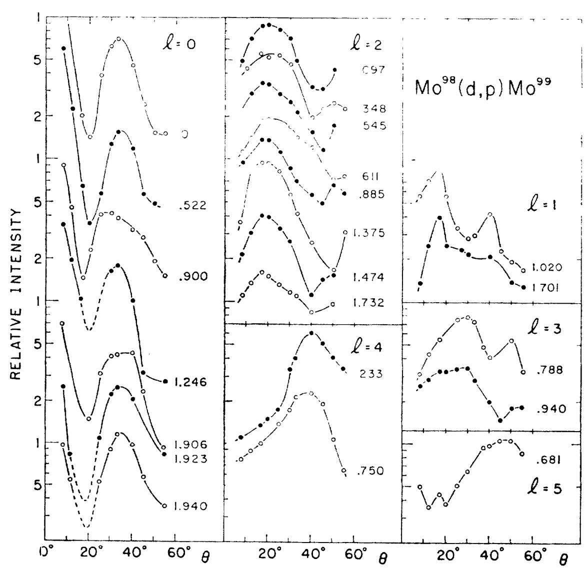

FIG. 8. $Mo^{98}(d,p)Mo^{99}$ angular distributions. See caption to Fig. 4.

Results for $Mo^{98}(d, p)Mo^{99}$ Reaction

Table IV summarizes the results for the $Mo^{98}(d, p)Mo^{99}$ reaction; the angular distributions are shown in Fig. 8. Using the results of (d, t) reaction on Mo^{100}, as was done for the other Mo isotopes, the 0.097- and 0.611-

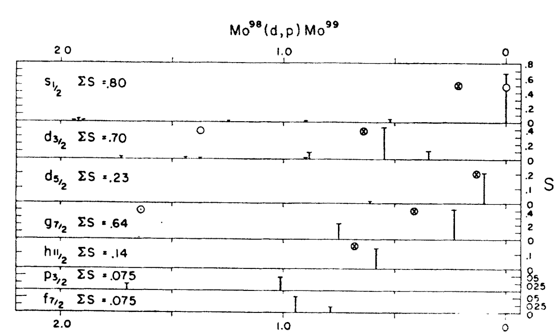

FIG. 9. Spectroscopic factors for $Mo^{98}(d,p)Mo^{99}$ reaction. See caption to Fig. 5.

TABLE IV. Levels in Mo^{99} from (d, p) reactions. See caption to Table II.

			Present work				Previous work[a]			
E (MeV)	l	j^{π}	$(d\sigma/d\Omega)(d, p)$ [b] (mb/sr)	$S(d, p)$	$S(d, t)$ [c]	$S(d, t)/S(d, p)$ [d]	E (MeV)	l	j^{π}	$S(d, p)$
0.0	0	$1/2^+$	7.49	0.67			0.0	0	$1/2^+$	0.64
0.097	2	$5/2^+$	2.44	0.21	1.0	4.7	0.100	2	$5/2^+$	0.23
0.233	4	$7/2^+$	0.622	0.42			0.222	(3)(4)	$7/2^+$	0.42
0.348	2	$3/2^+$	0.723	0.11	0.058	0.53	0.361	2	$3/2^+$	0.10
0.522	0	$1/2^+$	0.524	0.042						
0.545	2	$3/2^+$	2.98	0.43	0.28	0.65	0.545	2	$3/2^+$	0.35
0.611	2	$5/2^+$	0.226	0.018	0.13	7.2				
0.681	5	$11/2^-$	0.260	0.14			0.664	(4)(5)	$7/2^+$	0.35
0.750	(4)	$(7/2^+)$	0.355	0.22						
0.788	(3)	$(7/2^-)$	0.206	0.021			0.774	(2)	$3/2^+$	0.070
0.885	2	$3/2^+$	0.757	0.092	0.039	0.42				
	0	$1/2^+$	0.276	0.021			0.899	2	$3/2^+$	0.18
0.900										
	(2)	$(3/2^+)$	0.066	0.008						
0.940	3	$(7/2^-)$	0.545	0.054						
1.020	1	$(3/2^-)$	0.401	0.048						
1.246	0	$1/2^+$	0.120	0.008						
1.375	2	$3/2^+$								
(1.438)			0.051							
1.474	2	$3/2^+$								
1.528			0.181							
1.650										
1.701	1	$(3/2^-)$								
1.732	2	$(3/2^+)$								
1.790										
1.823										
1.906	0	$1/2^+$		0.018						
1.923	0	$1/2^+$								
1.940	0	$1/2^+$								

[a] See Ref. 4.
[b] Measured at first peak beyond 10°.
[c] Relative spectroscopic factor.
[d] Relative ratio.

MeV levels are assigned $j=\frac{5}{2}$. The remainder of the $l=2$ transitions are assigned $j=\frac{3}{2}$. These assignments are in agreement with the levels seen in Ref. 4. However, the 0.611-MeV level is here weakly excited and was not seen in Ref. 4. The state observed in Ref. 4 at 0.664 MeV, to be either $l=4$ or 5 and tentatively assigned to be $\frac{7}{2}^+$, is observed in this work as a $\frac{11}{2}^-$ state at 0.681 MeV with $l=5$. The spectroscopic factors for the (d, p) reactions leading to levels in Mo^{99} are plotted in Fig. 9.

Results for $Nb^{93}(d, p)Nb^{94}$ Reaction

Figure 10 shows the angular distributions of the proton peaks corresponding to levels in Nb^{94}. Table V summarizes the results. The seven transitions to Nb^{94} with excitation energies to 0.333 MeV having a transfer of $l=2$ are assigned a j transfer of $\frac{5}{2}$. The assignments are made using the knowledge that the ground state of Zr^{93} is a $d_{5/2}$ level and the remainder of the levels in Zr^{93}, which correspond to $l=2$ transitions,

TABLE V. Levels in Nb^{94} from (d, p) reactions. See caption to Table II. Also included are possible values of I_B.

	Present work					Previous work[a]	
E (MeV)	l	j^{π}	I_B	$(d\sigma/d\Omega)$ (d, p) [b] (mb/sr)	$S'(d, p)$	E (MeV)	I_B
0	2	$\frac{5}{2}^+$	(7)	2.44	0.22	0.0	6
0.041	2	$\frac{5}{2}^+$	(3)	0.90	0.081	0.041	(3)
0.058	2	$\frac{5}{2}^+$	(6)	1.33	0.12	0.058	
0.077	2	$\frac{5}{2}^+$	(4)	1.76	0.16	0.078	
	0	$\frac{1}{2}^+$		0.630	0.048		
0.113			5				
	2	$\frac{5}{2}^+$		1.92	0.17	0.113	
0.311	2	$\frac{5}{2}^+$	(2, 6)	0.229	0.020	0.314	
0.333	2	$\frac{5}{2}^+$	(2)	0.568	0.049	0.335	
0.628	2	$\frac{3}{2}^+$	3–6	0.395	0.059		
0.637	2	$\frac{3}{2}^+$	3–6	0.600	0.088	0.637	
0.791	2	$\frac{3}{2}^+$	3–6	0.061	0.009	0.794	
0.815						0.820	
0.932	2	$\frac{3}{2}^+$	3–6	0.178	0.025		
0.955	0	$\frac{1}{2}^+$	4, 5	3.11	0.24		
0.963						0.960	
	0	$\frac{1}{2}^+$		0.478	0.036		
1.003			4, 5			1.004	
	2	$\frac{3}{2}^+$		0.382	0.053		
1.058	0	$\frac{1}{2}^+$	4, 5	0.513	0.039	1.062	
	0	$\frac{1}{2}^+$		0.721	0.006		
1.165			4, 5			1.168	
	2	$\frac{3}{2}^+$		0.885	0.12		
1.202	4	$\frac{7}{2}^+$	2–8	0.061	0.052		
1.228	2	$\frac{3}{2}^+$	3–6	0.735	0.100	1.233	
1.255	2	$\frac{3}{2}^+$	3–6	0.176	0.024		
1.278	0	$\frac{1}{2}^+$	4, 5	1.38	0.11	1.278	
1.318	0	$\frac{1}{2}^+$	4, 5	1.69	0.13	1.324	
1.359	2	$\frac{3}{2}^+$	3–6	0.283	0.037		
1.390	2	$\frac{3}{2}^+$	3–6	0.175	0.023		
1.400	4	$\frac{7}{2}^+$	6–8	0.179	0.15	1.402	
1.498	1	$(\frac{3}{2}^-)$	3–6	1.01	0.043	1.496	
1.516	1	$(\frac{3}{2}^-)$	3–6	1.10	0.047		
1.567	0	$\frac{1}{2}^+$	4, 5	0.900	0.069	1.572	
	0	$\frac{1}{2}^+$		0.464	0.035		
1.618			4, 5			1.625	
	(2)	$(\frac{3}{2}^+)$		0.368	0.047		
1.662	(0)	$(\frac{1}{2}^+)$	4, 5	0.720	0.055	1.659	
1.693						1.693	
1.715						1.724	
	2	$\frac{5}{2}^+$		0.259	0.032		
1.777			5, 6			1.784	
	4	$\frac{7}{2}^+$		0.147	0.12		
1.805	2	$\frac{3}{2}^+$	3–6	0.538	0.067	1.808	

TABLE V. (*Continued*).

	Present work					Previous work[a]	
E (MeV)	l	j^{π}	I_B	$(d\sigma/d\Omega)\,(d,p)$ [b] (mb/sr)	$S'(d,p)$	E (MeV)	I_B
1.815	2	$\frac{3}{2}^+$	3–6	0.495	0.060		
1.857	0	$\frac{1}{2}^+$	4, 5	0.587	0.044	1.863	
	0	$\frac{1}{2}^+$		0.213	0.016		
1.930			4, 5				
	2	$\frac{3}{2}^+$		0.110	0.013		
1.969							
	0	$\frac{1}{2}^+$		0.124	0.010		
1.995			4, 5				
	2	$\frac{3}{2}^+$		0.064	0.007		
2.044	2	$\frac{3}{2}^+$	3–6	0.417	0.049		
						2.051	
2.056	2	$\frac{3}{2}^+$	3–6	0.754	0.089		
2.071	0	$\frac{1}{2}^+$	4, 5	0.331	0.026		
2.139						2.142	
2.191						2.190	
2.214	2	$\frac{3}{2}^+$	3–6	0.340	0.039		
	0	$\frac{1}{2}^+$		0.182	0.014		
2.236			4, 5				
	2	$\frac{3}{2}^+$		0.266	0.030		
2.253	2	$\frac{3}{2}^+$	3–6	0.358	0.041		
2.300	2	$\frac{3}{2}^+$	3–6	0.936	0.10	2.305	
2.320	0	$\frac{1}{2}^+$	4, 5	0.196	0.015		

[a] See Ref. 5.

[b] Measured at first peak beyond 10°.

are known $d_{3/2}$ levels.[3] A $d_{5/2}$ neutron should couple to the $g_{9/2}$ proton in the ground state of Nb^{93} in six different ways, yielding final spins from 2–7. Thus, there should be at least six closely spaced states which can have $d_{5/2}$ neutrons as part of their configurations. More are possible, since any state with positive parity in the final nucleus which has spin 2–7 can have at least one component due to a $d_{5/2}$ neutron. Thus, the first seven levels are assigned a component due to a $d_{5/2}$ neutron, because the nearest $d_{3/2}$ level in Zr^{93} is at 1.45 MeV.

For target nuclei such as Nb^{93}, where $I_A \neq 0$, S_{jk}' is given by Eq. (5). It was shown S_{jk}' has the same significance for spin-I_A targets as does S_{jk} for spin-0 targets. For the $l=2$ components of the first seven levels in Nb^{94}, S_j' [which is equal to U_j^2 by Eq. (7)] is 0.82. In Mo^{94} and Zr^{92}, which are isotones of Nb^{93}, $U_{5/2}^2$ is 0.76 and 0.54, respectively (see Ref. 3). Hence, it is unlikely that any of the strength of the $d_{5/2}$ single-particle state has been missed.

The fraction of strength which corresponds to each value of I_B is given by Eq. (6). Each state must be a definite spin I_B, but due to mixing with other configurations, there may be more than one state with the same value of I_B. In any case, the total strength of each single-particle level with the same value of I_B is given by Eq. (6). The angular distribution indicates that the 0.113-MeV level has a component due to an $s_{1/2}$ neutron and therefore must have $I_B=4$ or 5; hence, the assignments of I_B shown in Table V are made.

For the $g_{7/2}$ level, U^2 is 0.35 for Mo^{94}, 0.32

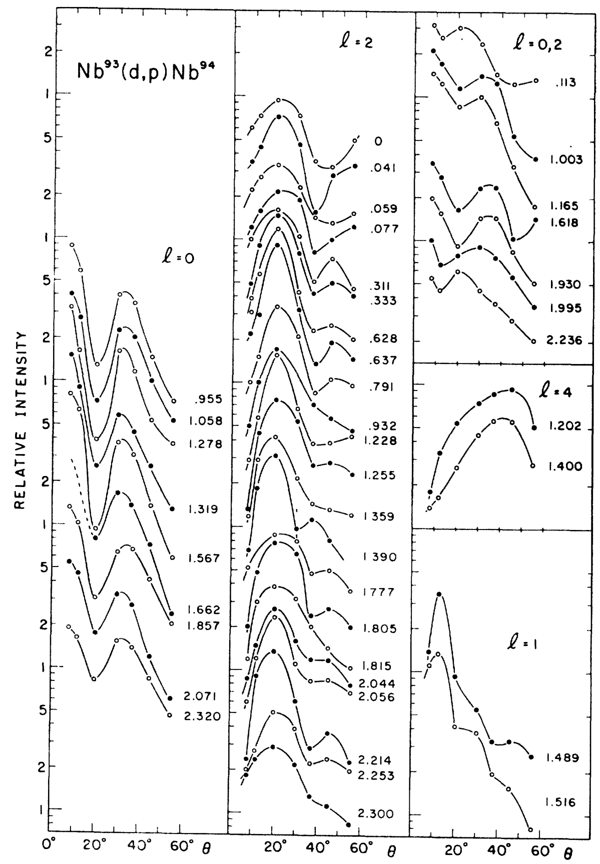

FIG. 10. $Nb^{93}(d,p)Nb^{94}$ angular distributions taken at angles of 8°, 12°, 20°, 30°, 37°, 45°, and 55°. See caption to Fig. 4.

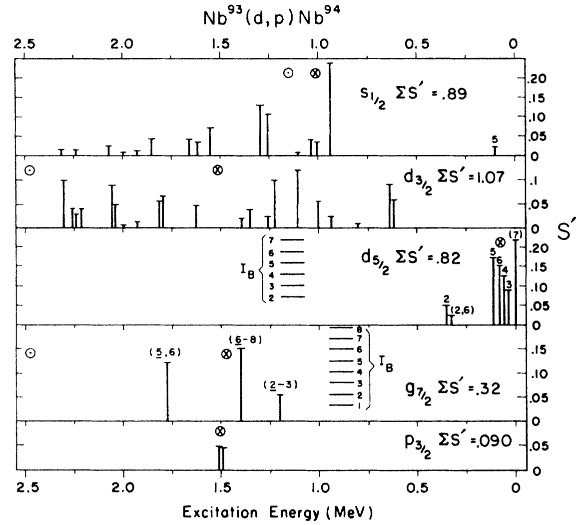

FIG. 11. Primed spectroscopic factors for $Nb^{93}(d,p)$ Nb^{94} reaction. See caption to Fig. 5. For the $g_{7/2}$ and $d_{5/2}$ levels the horizontal lines represent the maximum expected strength due to each value of I_B.

for Nb^{93}, and 0.92 for Zr^{92} (see Ref. 3). Apparently much of the $g_{7/2}$ strength has been missed in both $Mo^{94}(d,p)$ and $Nb^{93}(d,p)$. Coupling a $g_{7/2}$ neutron to a $g_{9/2}$ proton should yield eight configurations with spins from 1 to 8; however, only three levels corresponding to $g_{7/2}$ transitions are seen in Nb^{94}. The possible spins for the 1.202-, 1.400-, and 1.777-MeV

TABLE VI. Occupation numbers for the single-particle levels of the various nuclei listed.

Nucleus \ Level	$U_{1/2}{}^{+2}$	$U_{3/2}{}^{+2}$	$U_{5/2}{}^{+2}$	$U_{7/2}{}^{+2}$	$U_{11/2}{}^{-2}$
Zr^{91} [a]	0.96	1.00	0.89	0.97	
Mo^{93}	1.06	0.98	0.89	0.45	0.33
Mo^{93} [b]	1.15	1.00	0.940	0.493	
Zr^{93} [a]	1.13	1.01	0.54	0.92	
Nb^{94}	0.89	1.07	0.82	0.32	
Mo^{95}	0.80	0.95	0.76	0.35	0.26
Mo^{95} [b]	1.07	1.14	0.93	0.485	
Zr^{95} [a]	1.09	1.00	0.30	0.40	
Mo^{97} [b]	0.810	0.905	0.44	0.538	
Zr^{97} [a]	0.98	0.83		0.85	
Mo^{99}	0.80	0.70	0.23	0.64	0.14
Mo^{99} [b]	0.64	0.70	0.230	0.763	

[a] See Ref. 3.
[b] See Ref. 4.

TABLE VII. Centers of gravity of single-quasiparticle levels for various nuclei listed.

Nucleus	Center of gravity $s_{1/2}$	$d_{3/2}$	$d_{5/2}$	$g_{7/2}$	$h_{11/2}$
Zr^{91} [a]	1.55	2.70	0.0	2.70	
Mo^{93}	1.63	1.97	0.081	1.58	2.30
Mo^{93} [b]	1.65	2.58	0.149	2.32	
Zr^{93} [a]	1.15	2.40	0.0	2.4	
Nb^{94}	1.01	1.52	0.073	1.47	
Mo^{95}	1.28	1.98	0.222	1.19	1.93
Mo^{96} [b]	1.45	2.00	0.296	2.06	
Zr^{95} [a]	1.43	2.20	0.0	(2.6)	
Mo^{97} [b]	0.88	0.93	0.0	0.79	
Zr^{97} [a]	0.0	1.37		1.64	
Mo^{99}	0.22	0.64	0.132	0.41	0.68
Mo^{99} [b]	0.0	0.70	0.100	0.42	

[a] See Ref. 3.
[b] See Ref. 4.

levels of Nb^{94} are listed in Table V and are shown in Fig. 11. These assignments are made on the basis that $U_{7/2}{}^2$ should be similar in both Nb^{93} and Zr^{92}. The component of the 1.777 level due to a $d_{3/2}$ neutron limits the maximum value of I_B to 6 for that level. If there were no fragmentation of the $g_{7/2}$ level, the spins in italics in Table V would be those assigned to the three $g_{7/2}$ levels. However, fragmentation is likely since the $g_{7/2}$ level is fragmented into at least three states in Mo^{95}.

For the remainder of the states in Nb^{94}, the range over which I_B may extend is listed. The energy of levels in this work agree very well with other work.[5] A doublet (0.628, 0.637 MeV) which was not resolved in Ref. 5 is here resolved. Absolute cross sections

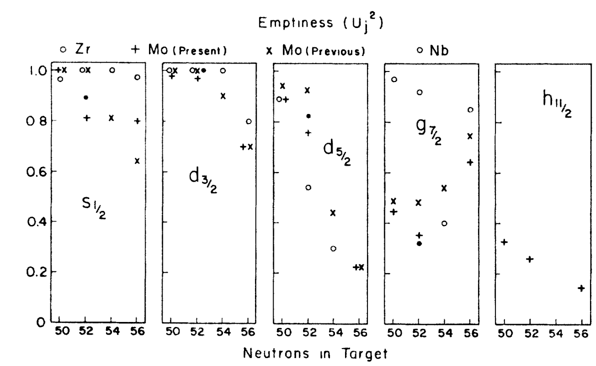

FIG. 12. Emptiness ($U_j{}^2$) of single-particle levels in various nuclei. See Table VI for references.

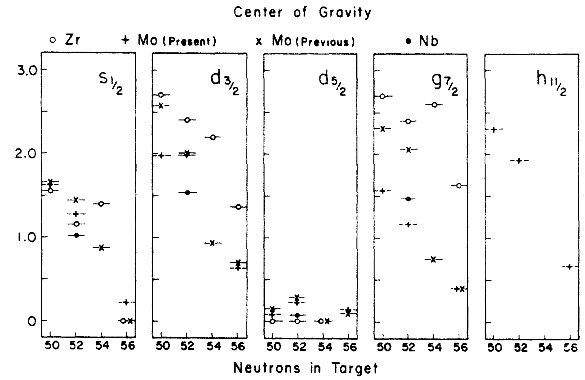

FIG. 13. Centers of gravity of levels in nuclei studied. See Table VII for references.

were not obtained in Ref. 5; hence no values of l were assigned. Sheline *et al.*[5] assigned the first two levels of Nb^{94} final spins of 6 and 3, respectively, based on the relative intensities of proton peaks obtained at several angles above 35°, and the assumption that the ground-state quintuplet was all $d_{5/2}$.

Figure 11 shows plots of S_{jk}' versus excitation energy for the levels of Nb^{94}. No $h_{11/2}$ state was observed in Nb^{94}, but the observed strength of this level in neighboring nuclei is such that the coupling of a $g_{9/2}$ proton and an $h_{11/2}$ neutron would leave the largest $h_{11/2}$ state with a maximum cross section of approximately 0.07 mb/sr. Hence, it is unlikely that any $h_{11/2}$ levels might be seen among the densely packed levels in Nb^{94} in the present experiment.

DISCUSSION

The results of this work are summarized in Tables VI and VII and shown in Figs. 12 and 13. Previous results for Mo (see Ref. 4) and Zr (see Ref. 3) are included in these tables and figures. Very good agreement is obtained between the present work and previous work for the $s_{1,2}$, $d_{3/2}$, and $d_{5/2}$ states of the Mo isotopes and the isotone Nb^{94}.

However, there are discrepancies in $U_{7/2}^2$ between the Zr isotopes and their isotones in Mo and Nb. It is possible that some $g_{7/2}$ strength has been missed in the $Mo^{94}(d, p)Mo^{95}$ reaction due to the high level density in Mo^{95}. Evidently some $g_{7/2}$ strength has been missed in the $Nb^{93}(d, p)Nb^{94}$ reaction, since eight states involving $g_{7/2}$ transitions should have been seen instead of the three, which were seen. Hence, $U_{7/2}^2$ should be considerably greater in Nb^{93}, and it is conceivable that it is larger in Mo^{94} too. The level density is small enough in Mo^{93}, that it is unlikely that any $g_{7/2}$ levels have been missed up to 3.2 MeV here; hence, it is improbable that the $g_{7/2}$ transition has much more strength in the $Mo^{92}(d, p)Mo^{93}$ reaction than has been found. It is also unexplainable why there is so much additional $g_{7/2}$ strength in the $Mo^{98}(d, p)Mo^{99}$ reaction than in the other $Mo(d, p)$ reactions.

The anomalous behavior of the $g_{7/2}$ levels in the isotopes of Pd, Cd, and In has already been reported[10] in conjunction with anomalous behavior of the $h_{11/2}$ levels. Lack of other data prohibits investigation of any anomalous behavior in the $h_{11/2}$ levels seen in this work. At present, work is being undertaken on isotopes of Ru to trace the behavior of the $g_{7/2}$ and $h_{11/2}$ levels as protons are added from the semiclosed 40-proton shell to the 50-proton closed shell.

---

[10] B. L. Cohen, R. A. Moyer, J. B. Moorhead, L. H. Goldman, and R. Diehl, Phys. Rev. **176**, 1401 (1968).